Available online at www.sciencedirect.com

ScienceDirect

Ceramics International 39 (2013) 9691–9697

CERAMICS INTERNATIONAL

www.elsevier.com/locate/ceramint

Short communication

Spark-plasma-sintering kinetics of ZrC–SiC powder mixtures subjected to high-energy co-ball-milling

Beatriz Núñez-González[a], Angel L. Ortiz[a,*], Fernando Guiberteau[a], Mats Nygren[b]

[a]Departamento de Ingeniería Mecánica, Energética y de los Materiales, Universidad de Extremadura, 06006 Badajoz, Spain
[b]Department of Materials and Environmental Chemistry, University of Stockholm, 10691 Stockholm, Sweden

Received 12 March 2013; received in revised form 9 April 2013; accepted 10 April 2013
Available online 17 April 2013

Abstract

The effect of SiC addition (5, 17.5, or 30 vol%) on the spark-plasma sinterability of ZrC ultra-high-temperature ceramics (UHTC) was investigated as a function of the intensity of high-energy co-ball-milling. It was found that the spark-plasma-sintering (SPS) kinetics of the ZrC–SiC powder mixtures is enhanced progressively with increasing co-milling time, which is due to the progressive refinement of the crystallite sizes. It was also found that in practice the SiC addition is beneficial for the SPS kinetics of ZrC if the co-milling time is short enough so as to refine the SiC crystallite size only to the submicrometre range, although the improvement in sinterability does not correlate with the SiC content. On the contrary, the SiC addition is increasingly detrimental for those co-milling times that promote SiC refinement to the nanoscale. This unexpected trend is due to slower ZrC crystallite size refinement in the presence of SiC and, especially, to the complex role played during SPS by the passivating SiO_2 films formed on the SiC particles, and is different from what has been observed in ZrB_2–SiC. Finally, implications of interest for the UHTC community are discussed.

Keywords: ZrC; High-energy ball-milling; Spark-plasma sintering; Ultra-high-temperature ceramics

1. Introduction

Zirconium carbide (ZrC), with a melting point of ~3450 °C, hardness of ~25–26 GPa, Young's modulus of ~400 GPa, thermal conductivity of ~20.5 W/m K, and electrical resistivity of $\sim 78 \times 10^{-6}$ Ω cm, to cite just some of its properties, is one of these few compounds catalogued as ultra-high-temperature ceramics (UHTCs), and is therefore a material of great interest in the world of extreme-environment engineering [1]. Unfortunately, ZrC UHTCs suffer from two important drawbacks, one being their poor sinterability due to the extremely-high melting point, and the other their low oxidation resistance due to the formation of porous oxide scales.

The problem of how to simultaneously improve the sinterability and oxidation resistance of UHTCs has been extensively investigated in ZrB_2. One possible solution is both to add SiC and to refine the coarse starting powders. This approach has also been tried in ZrC, although the utility of incorporating SiC as a sintering additive has yet to be fully validated because ZrC–SiC sintering studies have been few and far between and experimentally diverse. Thus, while Ma et al. [2] report a greater hot-pressing density (1900 °C, 30 MPa) for ZrC–20 vol% SiC than for ZrC [3], this comparison cannot be taken as conclusive due to the use of different ZrC powders. Those workers have also reported that the degree of densification attained by hot-pressing ZrC–SiC first increases and then decreases with SiC content [4], but the exact role of SiC is unclear because the powder mixtures used also contained 5 vol% graphite. Zhao et al. [5] find improved pressureless sintering of ZrC–20 vol% SiC composites at 1900 °C and 2100 °C, but prepared from ZrC, Si, and C mixtures, and therefore without using SiC. Zhao et al. [6] also describe the low-temperature densification (i.e., at 1800 °C) of ZrC–30 vol% SiC from that type of powder mixture, although now using spark-plasma sintering (SPS) and without reporting the comparison with a reference ZrC. Recently, Kljajević et al. [7] also described the spark-plasma sintering of ZrC–SiC powder mixtures prepared from $ZrSiO_4$, but the role of SiC is obscure due to the use of $LiYO_2$ sintering additive. Finally,

*Corresponding author. Tel.: +34 92 4289600x86726; fax: +34 92 4289601.
E-mail address: alortiz@materiales.unex.es (A.L. Ortiz).

0272-8842/$ - see front matter © 2013 Elsevier Ltd and Techna Group S.r.l. All rights reserved.
http://dx.doi.org/10.1016/j.ceramint.2013.04.033

Wang et al. [8] have densified ZrC–SiC composites at 1600 °C by reactive hot-pressing from ZrC and Si, but again the role of SiC is left unclear because the low-densification was assisted by Zr–Si liquid-phase formation. Other studies on ZrC–SiC composites report no sintering data.

Clearly, the findings of these few previous studies are insufficient for one to draw any definitive conclusion on whether or not SiC helps densify ZrC as it does for ZrB_2 [9]. Consequently, more sintering studies with a common experimental platform are required to unambiguously decide this question. Indeed, this is the objective of the present short communication, which aims to contribute to this end by investigating the SPS kinetics of ZrC–SiC powder mixtures as a function of their SiC content (5, 17.5, and 30 vol%) and intensity of high-energy co-ball-milling.

2. Experimental procedure

Commercially-available ZrC (Grade B, H.C. Starck, Germany; ~3 μm) and SiC (UF-15, H.C. Starck, Germany; ~0.55 μm) powders were combined in relative concentrations of 95–5, 82.5–17.5, and 70–30 vol% and were then shaker-milled (Spex D8000, Spex CertiPrep, USA) in air for different times in the interval 1–180 min with WC balls (6.7 mm diameter; Union Process Inc., USA) under a ball-to-powder weight ratio of 4. The ZrC crystallite sizes in the resulting powder mixtures were determined by X-ray diffractometry (XRD; D8-Advance, Brukers-AXS, Germany) [10]. Selected powders were also analysed by X-ray photoemission spectroscopy (XPS; K-Alpha, Thermo Scientific, UK) for chemical analysis.

The ZrC–SiC powder mixtures were spark-plasma sintered (Dr. Sinter SPS-2050, Sumitomo Coal Mining Co., Japan) in dynamic vacuum at 75 MPa pressure up to the temperature at which the graphite punches ceased travelling, with a limit of 2100 °C. The heating ramp was 100 °C min^{-1} up to 1200 °C, and 50 °C min^{-1} henceforth. The shrinkage curves logged were then corrected for the expansion of the graphite parts to obtain the real shrinkage curves of the powder mixtures themselves, followed by conversion to densification curves. Selected sintered materials were characterised using scanning electron microscopy (SEM; S-4800II, Hitachi, Japan).

3. Results and discussion

Fig. 1 shows the SPS-densification curves as a function of temperature for the three sets of ZrC–SiC powder mixtures. Qualitatively the shape of the curve is always the same, with a first linear part of moderate densification induced by mechanical compaction of the powder, followed by a second stretch of rapid densification, and lastly a third stretch of gradual densification towards the limiting value. Quantitatively, however, the densification curve depends on the co-milling time and SiC content.

It can be seen in Fig. 1 that the degree of densification at the onset of the SPS cycle first increases and then decreases with increasing co-milling time, which is the usual trend in

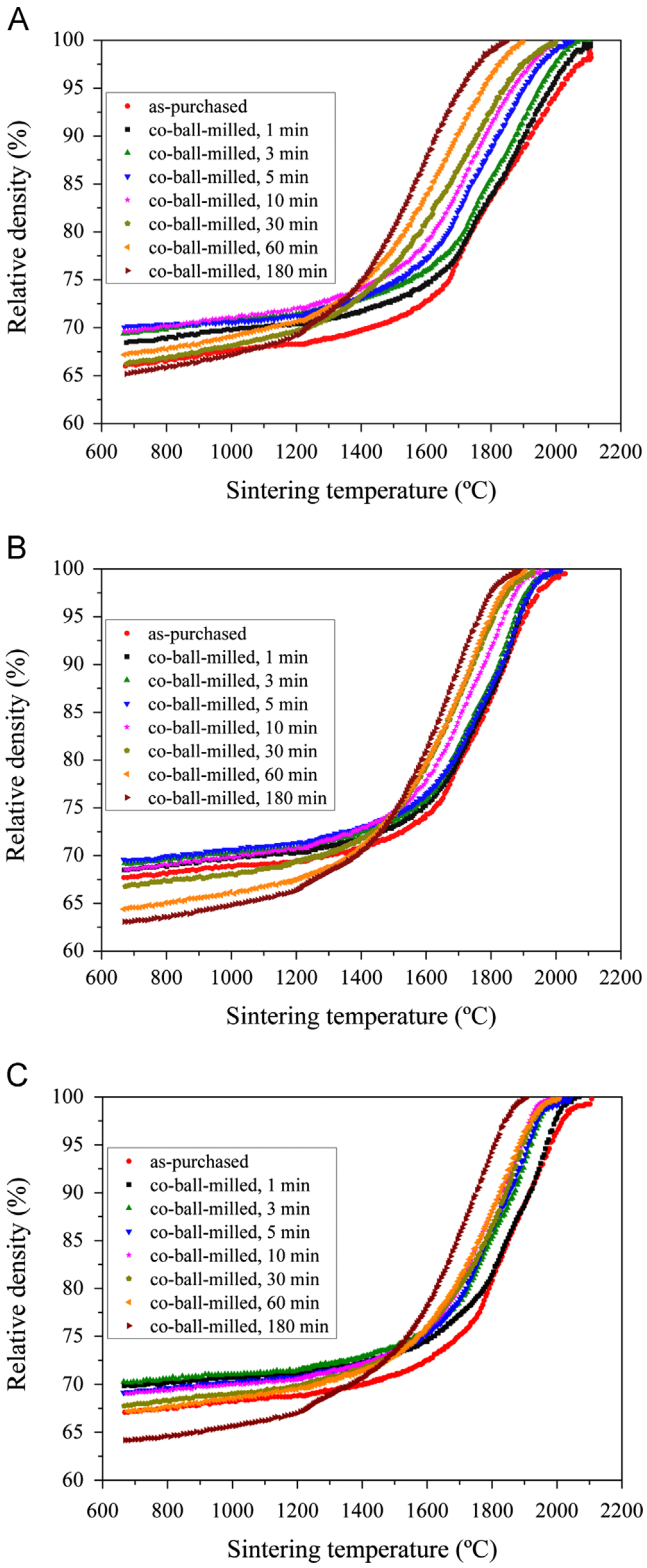

Fig. 1. SPS-densification curves as a function of temperature for the ZrC–SiC powder mixtures with different degrees of high-energy co-ball-milling and SiC additions of: (A) 5 vol%, (B) 17.5 vol%, and (C) 30 vol%.

ZrC [11] and ZrB_2 [12], and is due to the formation of hard agglomerates with nanometric sizes during milling. It is also immediately deduced from the shifting of the densification

curves towards lower temperatures that the SPS kinetics of the ZrC–SiC powder mixtures is improved with increasing co-milling time, a trend that is more pronounced for ZrC–5% SiC. The dependence of the sinterability of ZrC on the SiC content is, however, much more complex. Thus, comparison (not shown here) of the densification curves of ZrC–SiC powder mixtures with those reported before for pure ZrC [11] with the same milling time reveals first a shift towards lower temperatures with the SiC addition in the absence of co-milling and for short co-milling times (i.e., 3 min or less), especially for ZrC–17.5% SiC, and then a gradual change to a shift towards higher temperatures for longer co-milling times (i.e., >10 min) that is more marked with increasing SiC content. This suggests that only if no co-milling is used or if the co-milling time is short does SiC help in the SPS of ZrC; otherwise its addition is increasingly detrimental in terms of sinterability. The former is reasonable because SiC is less refractory and has smaller particle size in its starting condition than ZrC, and for the same reasons the latter is surprising; it can then be inferred that there should be at least another mechanism operating that gradually reduces the beneficial effect of the SiC addition with the progressive co-milling and that eventually becomes even dominant thus impoverishing the sinterability.

A detailed analysis of the densification curves confirms the conclusions inferred from the cursory inspection of Fig. 1. Thus, it can be seen in Fig. 2 that for a given SiC content the onset temperatures of the early (T_{OES}), intermediate (T_{OIS}), and final (T_{OFS}) sintering regimes, and the temperature of the change to grain-boundary diffusion (T_{GBD})[1] all decrease, first abruptly and then more gradually, with increasing co-milling time. This is a clear sign that the SPS kinetics of the ZrC–SiC powder mixtures benefit from the progressive co-milling, although their improvement beyond 3 h of co-milling will only be slight, so that such prolonged co-millings are not very practical. The trend with the SiC content is substantially different, and, as was to be expected, very complex. It can be seen in Fig. 2 that, except for T_{OES} which decreases with increasing SiC content, the rest of the characteristic temperatures increase systematically as the SiC content increases when the co-milling time is moderate or long (i.e., >3 min). This is a sign of impoverished sinterability. However, when the co-milling time is short (i.e., <3 min), the SiC addition is to a greater or lesser extent beneficial for the sinterability, although without any direct correlation with the SiC content since ZrC–17.5% SiC exhibits better kinetics than ZrC–5% SiC and ZrC–30% SiC.

[1]The early stage of sintering is the sintering regime where there occurs the formation and rapid growth of necks among particles, recognised by the deviation of the densification curve from the linear compaction stretch. The intermediate stage of sintering is the sintering regime where the pore distribution transforms from open porosity to closed porosity, beginning typically at ~75% relative density [13]. The final stage of sintering is the sintering regime where the closed porosity is eliminated, starting typically at ~90% relative density [13]. The change from surface diffusion to grain-boundary diffusion is evidenced by a maximum in the time derivative of the shrinkage curve [14].

The improvement in sinterability with increasing co-milling time was to be expected because, as shown in Fig. 3, the high-energy ball-milling progressively refined the crystallite size, or size of the primary particles because the refinement occurs by brittle fracture [11], to the nanoscale. In non-oxide ceramics, this refinement is accompanied by surface passivation, but even so the shortening of the diffusion distances and the formation of a greater density of grain boundaries available as fast diffusion paths speed up the sintering kinetics in accordance with Herring's scaling law [15].

On the contrary, the impoverishment in sinterability with increasing SiC addition for moderate or long co-milling times was surprising because it is not what is observed in ZrB_2, whose SPS kinetics is substantially accelerated if co-milled with SiC [16]. A first possible interpretation of this unexpected effect with the SiC addition, as SiC is less refractory than ZrC and its addition without co-milling indeed improved the sinterability, would lie in the slowing down of the kinetics of crystallite size refinement of ZrC that occurs with SiC addition (see Fig. 3). This is also the case in ZrB_2, and has been attributed to the combination of the earlier SiC nano-crystallization promoted by its greater brittleness and the decreased ball-to-powder volume ratio resulting from the lower SiC density [17]. Whatever the mechanism in ZrC, for the scope of the present investigation it is sufficient to consider that, in accordance with Herring's scaling law, the kinetics of interparticle diffusion controlled sintering is slower with increasing crystallite size. Nevertheless, although the greater ZrC crystallite size may contribute to the effect, plots of the characteristic temperatures against crystallite size, such as that of T_{OFS} in Fig. 4, indicate that alone it is insufficient to account for the observed impoverishment in sinterability. Instead, an additional mechanism of kinetics impoverishment has to be operating in the ZrC–SiC powder mixtures subjected to moderate and, above all, long co-milling times for which the crystallite sizes converge gradually to the same limiting value.

This second mechanism is most likely related to the oxygen impurities in the powders, and in particular to the SiO_2 formed on the SiC particles. This is because the sought mechanism has to increase in importance both with increasing SiC content and with decreasing crystallite size–a combination of requirements fulfilled by SiO_2 as confirmed by the XPS analyses in Fig. 5, but not by ZrO_2 (whose abundance of course decreases as the SiC content increases because of the lower ZrC content). In SPS, whether these SiO_2 impurities help or hinder densification depends on the outcome of the competition between two opposing tendencies. First, the surface SiO_2 favours evaporation–condensation or surface diffusion mass transport mechanisms at moderate temperatures [18], which is detrimental to densification because surface energy is consumed in promoting microstructural coarsening. Indeed, SiC is a typical example of a material that forms sinter bonds between particles without densification, which is why SiC powders are doped with B and C to promote their solid-state sintering [19] or with other additives for their liquid-phase sintering [20]. And second, at higher temperatures the surface SiO_2 will segregate under the applied pressure at multi-grain joints because the more

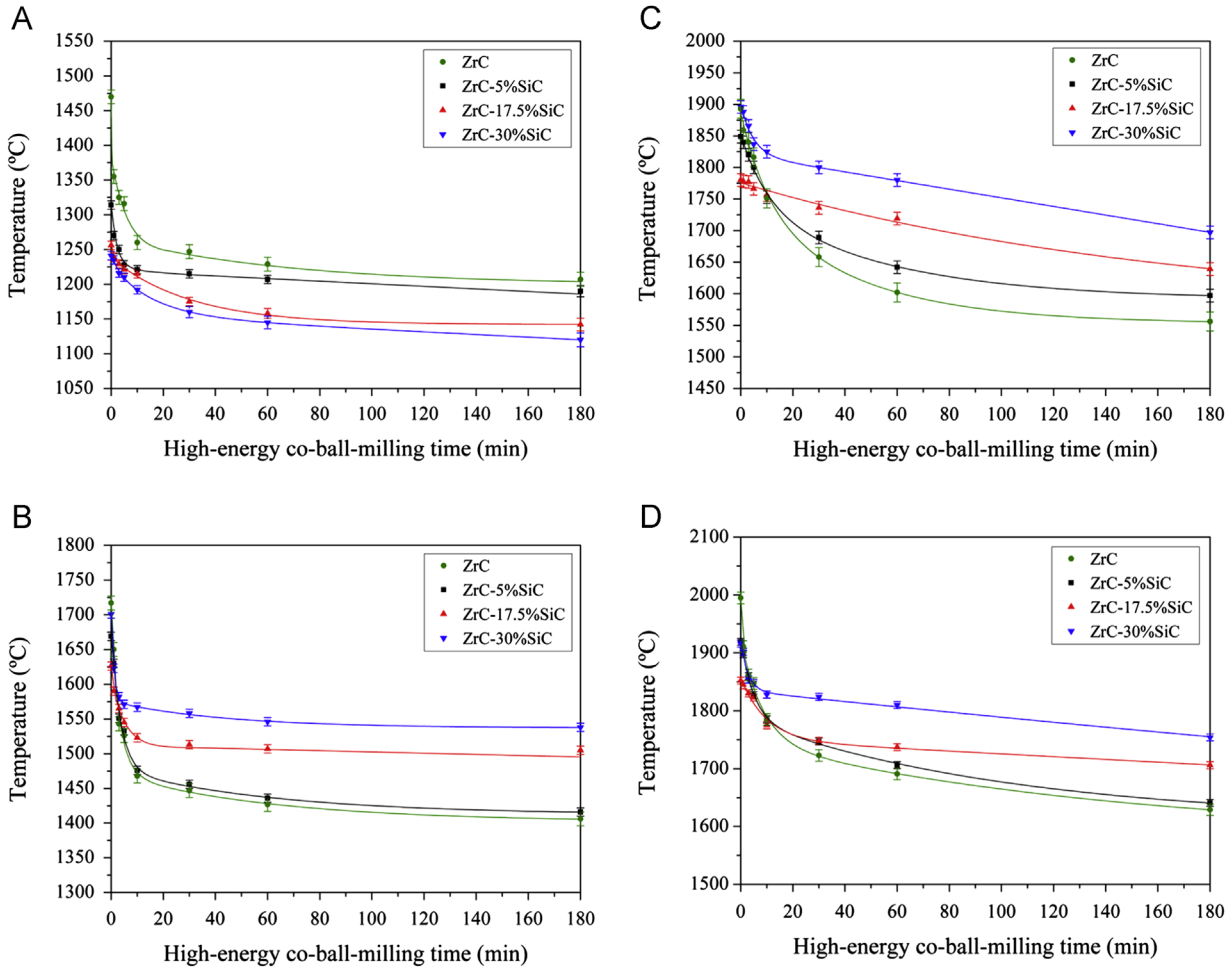

Fig. 2. Evolution of (A) T_{OES}, (B) T_{OIS}, (C) T_{GBD}, and (D) T_{OFS} with high-energy ball-milling time for the ZrC powder (taken from [11]) and ZrC–SiC powder mixtures (5, 17.5, or 30 vol% SiC). The points are the experimental data, and the lines are merely to guide the eye.

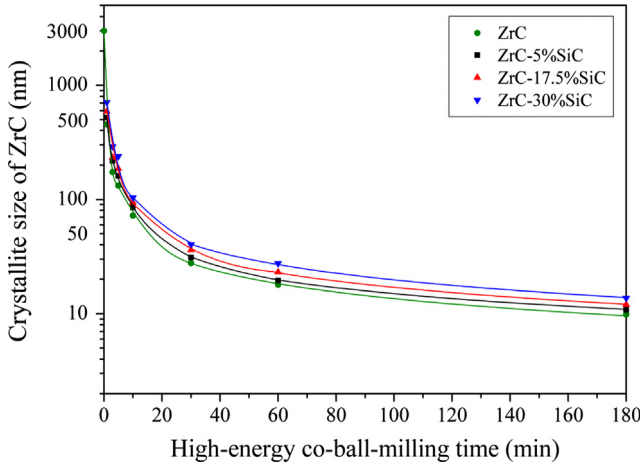

Fig. 3. Average size of the ZrC crystallites as a function of high-energy ball-milling time, determined by XRD. The points are the experimental data, and the lines are merely to guide the eye. The crystallite size in the as-purchased condition was taken to be the same as the particle size measured by electron microscopy.

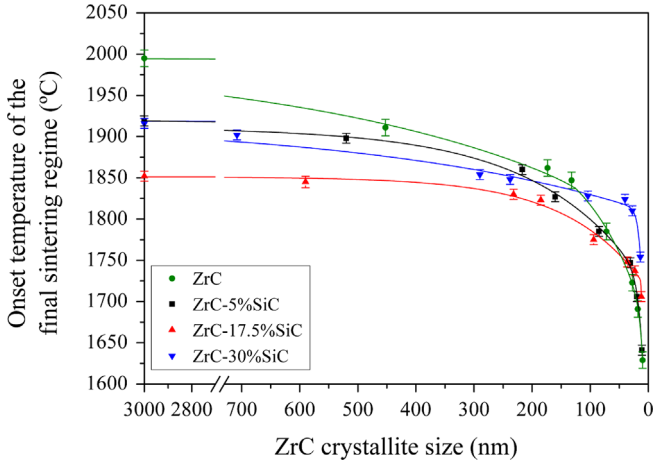

Fig. 4. Dependence of T_{OFS} on the crystallite size of ZrC achieved during the high-energy ball-milling for the ZrC powder (taken from [11]) and ZrC–SiC powder mixtures (5, 17.5, or 30 vol% SiC). The points are the experimental data, and the lines are merely to guide the eye.

refractory ZrO_2 does [21]. This is beneficial for densification because it fills pores. Considering the experimental results shown in Fig. 2, one may reasonably conclude that the balance is increasingly tipped in favour of microstructural coarsening with increasing SiC content due to the greater SiO_2 abundance. Furthermore, this trend is exacerbated by the fact that the

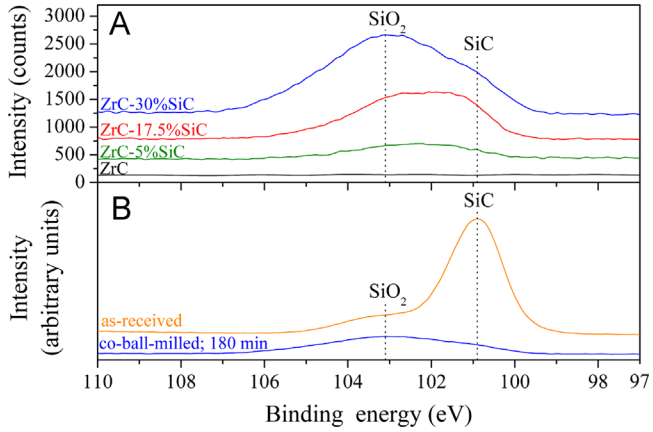

Fig. 5. High-resolution XPS spectra of the Si 2p (doublet Si $2p_{3/2}$–$2p_{1/2}$) core level for (A) the ZrC powder and ZrC–SiC powder mixtures (5, 17.5, or 30 vol % SiC) with 180 min of milling, and (B) the ZrC–30% SiC powder mixture in the as-received condition and ball-milled for 180 min. The peak indexing for the two bonding statuses observed for the Si atoms is included. The spectra in (A) have been shifted along the vertical axis to facilitate their comparison. In (B), they have also have been normalised by imposing the same intensity for the Si peak associated with SiO_2.

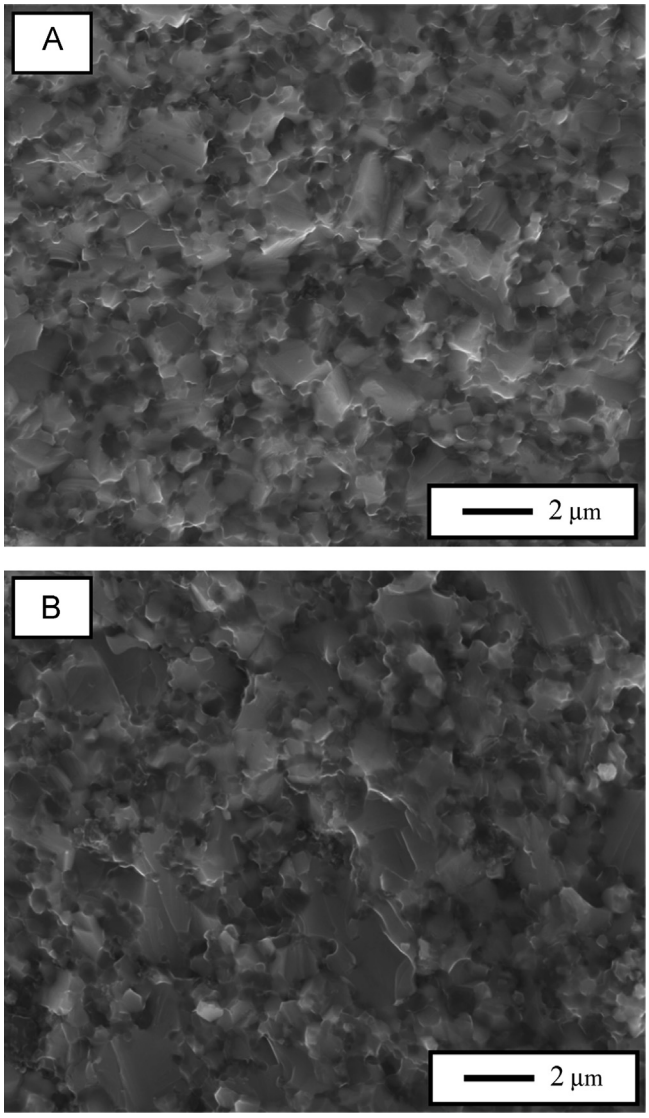

Fig. 6. Low-magnification SEM micrographs of the UHTCs resulting from the SPS at 1900 °C without soaking, of (A) ZrC–17.5%SiC and (B) ZrC–30%SiC powder mixtures with 180 min of high-energy co-ball-milling. Smaller grains are SiC and oxides; larger grains are ZrC. Darker areas are not pores, as was confirmed by higher-magnification observations. Owing to their lower SPS temperature of 1850 °C, the SEM images of the ZrC powder and of the ZrC–SiC powder mixtures with the same milling conditions are not presented to avoid a biased comparison.

ZrC–SiC powder mixtures have an earlier onset of evaporation-condensation/surface diffusion (Fig. 2A) but a delayed activation of grain-boundary diffusion (Fig. 2D) with increasing SiC content, which increases the exposure times to temperatures at which coarsening is more significant. The SEM micrographs in Fig. 6 confirm the greater coarseness of the ZrC grains with increasing SiC content for an identical SPS cycle. This explanation would also account for the observation that ZrC–5% SiC benefits more from the milling than ZrC–17.5% SiC and ZrC–30% SiC.

The scenario for short co-milling times is different. In this case, it appears that the combination of microstructural coarsening and larger ZrC crystallite size is not the predominant factor in conditioning the SPS kinetics, which indeed benefit from the SiC addition although gradually less as the short milling time increases mainly due to the increasing introduction of SiO_2. This is attributable to the lower content of oxide impurities introduced into the powder mixtures when SiC is refined only to the submicrometric range, because the XRD measurement of the SiC crystal size above 3 min of co-ball-milling is at the nanoscale. This finding is consistent with independent observations on ZrC–SiC UHTCs pressureless-sintered from powders also refined to the submicrometre scale (~0.5 μm) [5]. However, there seems to be some complex competition between mechanisms, with the small (i.e., 5 vol%) and substantial (i.e., 30 vol%) SiC additions being worse than the moderate addition (i.e., 17.5 vol%). This clearly merits future investigation because one infers that there exists an optimal SiC content that offers the best trade-off between the benefits and drawbacks of SiO_2 impurities. Again, this deduction is consistent with independent observations on hot-pressed ZrC–SiC UHTCs with 10, 20, and 30 vol% SiC [4].

The important lesson that can be learnt from this study is that the SiO_2 introduced during the co-milling of ZrC and SiC is detrimental for the sinterability of these UHTCs because it results in lesser improvement in sinterability when co-milling time is sufficiently short and in impoverishment when the co-milling time is moderate or large. As SiO_2 comes exclusively from the surface passivation of SiC, or in other words without SiC there is no SiO_2, it could also be said that in practice the SiC addition is detrimental to the densification of ZrC if the SiC has nanometric particle sizes and therefore carries abundant SiO_2, but will act as an effective sintering additive if its particle size is intentionally controlled to stay within the submicrometric range and thus to carry less SiO_2. Therefore, the preparation of ZrC–SiC composite nanopowders is in

general inadvisable in terms of sinterability, especially by high-energy co-ball-milling due to the slower kinetics of crystallite size refinement of ZrC. In principle, this conclusion should be valid not only for SPS, but also for hot-pressing and pressureless sintering because the combination of lower compaction pressures and slower heating ramps will further favour coarsening. Alternatively, since the bane of nano-SiC is its surface SiO_2, it might be found to be an efficient sintering additive for ZrC if it were appropriately purified to remove surface oxide, or if it were added in combination with other compounds that promote the carbothermal-reduction of oxide during sintering. Further investigation into these aspects is warranted because the incorporation of SiC into ZrC matrices would indeed be beneficial for the material's properties, such as its resistance to oxidation, and there is clear interest today in the development of UHTC nanocomposites.

Finally, it is worth mentioning that the ZrC case is clearly different from that of ZrB_2, for which SiC substantially accelerates the SPS kinetics [16], regardless of the high-energy co-milling conditions (and therefore of the crystallite sizes). The difference lies in the fact that in ZrB_2 the passivating B_2O_3 and SiO_2 films react during SPS to form a low-viscosity liquid borosilicate that both speeds up interparticle diffusion and is segregated under pressure into the multi-grain joints, thus filling up the pores [16]. This is not possible in ZrC because it passivates to form only ZrO_2, and the first liquid in the ZrO_2–SiO_2 binary system does not occur until 1678 °C [22]. Thus, another lesson that is learnt from this study is that what works for a subfamily of the UHTCs (i.e., borides) does not necessarily work for the others (i.e., carbides, and probably nitrides too).

4. Conclusions

We have investigated the SPS kinetics of ZrC–SiC powder mixtures subjected to different intensities of high-energy co-ball-milling as a function of SiC content (5, 17.5, or 30 vol%). The results allow the following conclusions to be drawn:

1. The high-energy co-ball-milling progressively enhances the spark-plasma sinterability of the ZrC–SiC UHTCs due to the refinement of the crystallite sizes which reduces the diffusion distances and develops a greater density of grain boundaries available as faster diffusion paths.
2. The SiO_2 introduced during co-milling as the passivating layer on the SiC particles is detrimental for the sinterability of ZrC–SiC because it results in lesser improvement in sinterability when the co-milling time is short and in impoverishment for moderate or large co-milling times. The slowing down of the kinetics of crystallite size refinement of ZrC that occurs during co-milling with SiC also contributes to further impoverish the sinterability. In this way, in practice the SiC addition enhances the SPS kinetics of ZrC only if the co-milling time is short enough so as to refine the SiC crystallite size to just the submicron range, where the surface SiO_2 impurities do not yet condition the sinterability entirely; otherwise, SiC addition is detrimental, essentially because it dominates the microstructural coarsening promoted by the surface SiO_2 on the SiC nanoparticles.
3. Unlike the case with ZrB_2, SiC cannot be considered a general sintering additive for ZrC, although it may act efficiently if an appropriate strategy is used to prepare the powder. The key aspect is either to control the SiC particle size, to thus modulate the SiO_2 content introduced, in which case there does appear to exist an optimal content of SiC additive because logically this also dictates the total SiO_2 content, or alternatively to be able to remove the surface SiO_2 from the SiC particles for a greater exploitation of the beneficial effect of their addition.

Acknowledgements

This work was supported by the Ministerio de Ciencia y Tecnología (Government of Spain) and FEDER funds under Grant no. MAT 2010-16848.

References

[1] E. Wuchina, E. Opila, M. Opeka, W. Fahrenholtz, I. Talmy, UHTCs: ultra-high temperature ceramic materials for extreme environment applications, Interface 16 (4) (2007) 30–36.
[2] B. Ma, X. Zhang, J. Han, W. Han, Microstructure and mechanical properties of ZrC–SiC–Cg ceramic prepared by hot pressing, Rare Metal Materials and Engineering 38 (2) (2009) 890–893.
[3] P. Barnier, C. Brodhag, F. Thevenot, Hot-pressing kinetics of zirconium carbide, Journal of Materials Science 21 (7) (1986) 2547–2552.
[4] B. Ma, X. Zhang, J. Han, W. Han, Fabrication of hot-pressed ZrC-based composites, Proceedings of the Institution of Mechanical Engineers, Part G: Journal of Aerospace Engineering 223 (2009) 1153–1157.
[5] L. Zhao, D. Jia, X. Duan, Z. Yang, Y. Zhou, Pressureless sintering of ZrC-based ceramics by enhancing powder sinterability, International Journal of Refractory Metals and Hard Materials 29 (4) (2011) 516–521.
[6] L. Zhao, D. Jia, X. Duan, Z. Yang, Y. Zhou, Low temperature sintering of ZrC–SiC composite, Journal of Alloys and Compounds 509 (2011) 9816–9820.
[7] L. Kljajević, S. Nenadović, M. Nenadović, D. Gautam, T. Volkov-Husović, A. Devečerski, B. Matović, Spark plasma sintering of ZrC–SiC ceramics with $LiYO_2$ additive, Ceramics International 39 (5) (2013) 5467–5476.
[8] X.-G. Wang, G.-J. Zhang, J.-X. Xue, Y. Tang, X. Huang, C.-M. Xu, P.-L. Wang, Reactive hot pressing of ZrC–SiC ceramics at low temperature, Journal of the American Ceramic Society 96 (1) (2013) 32–36.
[9] S.S. Hwang, A.L. Vasiliev, N.P. Padture, Improved processing and oxidation resistance of ZrB_2 ultra-high temperature ceramics containing SiC nanodispersoids, Materials Science and Engineering A 464 (1–2) (2007) 216–224.
[10] F. Sánchez-Bajo, A.L. Ortiz, F.L. Cumbrera, Analytical formulation of the variance method of line-broadening analysis for voigtian X-ray diffraction peaks, Journal of Applied Crystallography 39 (4) (2006) 598–600.
[11] B. Núñez-González, A.L. Ortiz, F. Guiberteau, M. Nygren, Improvement of the spark-plasma-sintering kinetics of ZrC by high-energy ball-milling, Journal of the American Ceramic Society 95 (2) (2012) 453–456.
[12] V. Zamora, A.L. Ortiz, F. Guiberteau, M. Nygren, Crystal-size dependence of the spark-plasma-sintering kinetics of ZrB_2 ultra-high-temperature ceramics, Journal of the European Ceramic Society 32 (2) (2012) 271–276.
[13] R.M. German, Sintering Theory and Practice, Wiley, New York, 1996.
[14] Z. Shen, M. Nygren, Microstructural prototyping of ceramics by kinetic engineering: applications of spark plasma sintering, Chemical Record 5 (3) (2005) 173–184.

[15] C. Herring, Effect of change of scale on sintering phenomena, Journal of Applied Physics 21 (1950) 301–303.
[16] V. Zamora, A.L. Ortiz, F. Guiberteau, M. Nygren, On the enhancement of the spark-plasma-sintering kinetics of ZrB_2–SiC powder mixtures subjected to high-energy co-ball-milling, Ceramics International 39 (4) (2013) 4191–4204.
[17] V. Zamora, A.L. Ortiz, F. Guiberteau, L.L. Shaw, M. Nygren, On the crystallite size refinement of ZrB_2 by high-energy ball-milling in the presence of SiC, Journal of the European Ceramic Society 31 (13) (2011) 2407–2414.
[18] W. van Rijswijk, D.J. Shanefield, Effects of carbon as a sintering aid in silicon carbide, Journal of the American Ceramic Society 73 (1) (1990) 148–149.
[19] S. Prochazka, R.M. Scanlan, Effect of boron and carbon on sintering of SiC, Journal of the American Ceramic Society 58 (1–2) (1975) 72.
[20] F. Rodríguez-Rojas, A.L. Ortiz, F. Guiberteau, M. Nygren, Oxidation behaviour of pressureless liquid-phase-sintered α-SiC with additions of $5Al_2O_3$+$3RE_2O_3$ (RE=La, Nd, Y, Er, Tm, or Yb), Journal of the European Ceramic Society 30 (15) (2010) 3209–3217.
[21] V. Zamora, A.L. Ortiz, F. Guiberteau, M. Nygren, In-situ formation of ZrB_2–ZrO_2 ultra-high-temperature composites from high-energy ball-milled ZrB_2 powders, Journal of Alloys and Compounds 518 (2012) 38–43.
[22] W.C. Butterman, W.R. Foster, Zircon stability and ZrO_2–SiO_2 phase diagram, American Mineralogist 52 (5–6) (1967) 880–885.